Micellization and the Surface Hydrophobicity of Amphiphilic Poly(vinylphenol)-*block*-Polystyrene Block Copolymers

Pao-Hsaing Tung, Shiao-Wei Kuo,*Shih-Chien Chan, Chih-Hao Hsu, Chih-Feng Wang, Feng-Chih Chang*

The self-assembly of PVPh-*b*-PS in different solvents was studied. Upon replacing toluene by THF as the solvent, the morphology of the resulting aggregates change from core-shell spheres, rod-like micelles and vesicles to onion-like aggregates. With increasing block copolymer concentration, morphologies such as honeycomb-like films, surfaces of aggregated large porous spheres, or pincushion-like spheres with protruding tubular vesicle aggregates are observed. These surface-patterned films show significantly enhanced hydrophobicity. The results suggest that a superhydrophobic behavior can be achieved, with a maximum contact angle of 158°, by using the pincushion-like micellar structure.

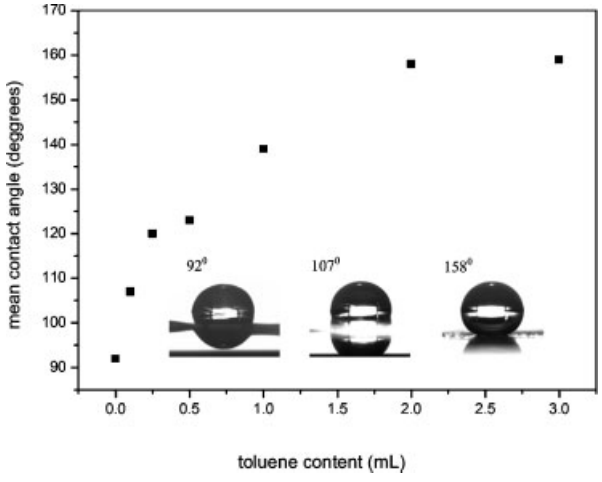

Introduction

The design of highly ordered supramolecular architectures in solution and superhydrophobic thin film surfaces has attracted considerable attention in the past decade because of their great advantage in both basic research and industrial applications. Micellar nanostructures have been used, for instance, as drug carriers in delivery system[1–3] or as templates for nanotechnology.[4,5] In addition, the superhydrophobic surface thin films with water repellency also have wide applications in daily life as well as in industrial process.[6,7]

Amphiphilic block copolymers dissolved in a selective solvent for one block can exhibit complex self-assembling behavior of supramolecular structures such as spheres, cylinders, lamellae, vesicles, and other mesoscopic aggregates.[8–12] These micelles are generally pictured as nano-objects with two concentric regions: a core consisting of an insoluble part of amphiphilic block copolymers, and a corona of soluble part swollen in the selective solvent. The block copolymer micellar systems are more

P.-H. Tung, S.-C. Chan, C.-H. Hsu, F.-C. Chang
Institute of Applied Chemistry, National Chiao-Tung University, Hsin-chu, Taiwan
Fax: +886 3 513 1512; E-mail: changfc@mail.nctu.edu.tw
S.-W. Kuo
Department of Materials and Optoelectronic Engineering, National Sun Yat-Sen University, Kaohsiung, Taiwan
E-mail: kuosw@mail.nsysu.edu.tw
C.-F. Wang
Department of Materials Science and Engineering, I-Shou University, Kaohsiung, Taiwan

DOI: 10.1002/macp.200700078

stable than low molecular weight surfactant micelles due to the presence of a long chain of insoluble part of amphiphilic block copolymers, and additionally amphiphilic block copolymer micelles can be further stabilized by crosslinking the latter. Two types of micelles can be distinguished in block copolymer solutions: one is star-like micelles and the other is crew-cut aggregates. Star-like micelles are also called "long-hair", which are formed by block copolymers with relatively long corona, but short core blocks. Based on our knowledge, star-like micelles from block copolymers in solution are generally spherical, but still only a few are non-spherical star-like micelles.[13–16] On the contrary, crew-cut micelles represent a new type of aggregates and more complex morphologies than star-like micelles, which have received much attention in recent years.[17–20] They are formed by highly asymmetric block copolymers, where the insoluble core is bulky and has much longer chains than the soluble forming blocks. Usually, stable crew-cut aggregates can be prepared in a solvent mixture either by direct dissolution or by dissolving first the copolymer in a good solvent for both blocks and then adding the poor solvent in one of the blocks of the copolymer. This kind of morphology is influenced by many variables, such as the initial copolymer concentration in solution, the nature of the common solvent, the type and concentration of added ions (such as salt, acid, or base), the amount of selective solvent, because the micellar morphologies are mainly controlled by a force balance between the stretching of the core forming blocks, the interfacial energy between the core and the outside solvent, and the repulsive interaction among corona chains.[19]

Micellar aggregates can be formed as fractured structures or highly ordered architecture on the surface, which display special water repellency.[21–23] Surface wettability is governed by both the chemical composition and the surface structure.[24–27] Increase in the surface roughness of hydrophobic materials can dramatically enhance the surface water repellency. Usually, a superhydrophobic surface is defined as having a water contact angle (CA) over 150°. In nature, the lotus-leaf is a well-known example of superhydrophobic surface with micro–nano two-length scale hierarchical structure even without any particularly low surface energy materials. As a result, many previous works have reported the superhydrophobic surface by mimicking natural lotus-like micro-nano-binary structure (MNBS).[21] However, it is still important and remains a challenge to practice the application of a superhydrophobic surface in a large area.

In this paper, we will report micellization behavior and water repellency of an amphiphilic block copolymer of poly(vinylphenol)-*block*-polystyrene (PVPh-*b*-PS). The aggregates of the diblock copolymer were dissolved in THF solution with various copolymer concentrations (2–50 $mg \cdot mL^{-1}$), and selective toluene solvent was added to induce aggregation of the PVPh block. When the initial copolymer concentration is highly concentrated, various complexed morphologies can be observed including nanoscaled crew-cut aggregates,[28] mesoscaled structures of honeycomb-patterned and pincushion-like aggregates. In this study, the wettability of copolymer films containing various contents of the crew-cut aggregates by adjusting the toluene content is investigated.

Experimental Part

Materials

Styrene (Aldrich, 99%) and 4-*tert*-butoxystyrene monomers (*t*BOS, Aldrich, 99%) were distilled from finely ground CaH_2 before use. *Sec*-butyllithium (Acros, 1.3 M in cyclohexane) was used as the initiator for anionic polymerization. Tetrahydrofuran (THF), which was used as polymerization solvent for anionic polymerization, was purified by distillation under argon from the red solution obtained by diphenylhexyllithium (produced by the reaction of 1,1-diphenylethylene and BuLi).

Synthesis of a Block Copolymer

The poly(4-*tert*-butoxystyrene)-*block*-polystyrene (P*t*BOS-*b*-PS) diblock copolymer was synthesized by sequential living anionic polymerization under inert atmosphere[29] in THF at −78 °C using 1.3 M *sec*-butyllithium in cyclohexane as the initiator. The *t*BOS monomer was polymerized first for 2 h, and an aliquot of the poly(*t*BOS) sample was withdrawn for analysis after termination with degassed methanol. The styrene monomer was then added to the reactor and the reaction was terminated with degassed methanol after 2 h. The resulting P*t*BOS-*b*-PS diblock copolymer product was dissolved in dioxane and then a ten-fold excess of concentrated HCl was added to the solution. The hydrolysis reaction was carried out overnight at 85 °C under argon atmosphere and the resultant product was precipitated in a methanol/water mixture (2:8, v/v).[30] After neutralization with 10 wt.-% NaOH solution to a pH value of 6–7, the crude copolymer product was filtered, followed by two dissolved (THF)/precipitate (methanol/water) cycles and finally purified by the Soxhlet extraction with water for 72 h before being dried under vacuum at 80 °C. The chemical mechanism to synthesize the PVPh-*b*-PS diblock copolymer is shown in Scheme 1.

Micellization Procedures

The crew-cut aggregates with PS coronas and PVPh cores were obtained by a dialysis method. The block copolymer (2 $mg \cdot mL^{-1}$) was first dissolved in THF, which is a good solvent suitable for both copolymer blocks. Subsequently, a given volume of toluene was added gradually into the polymer THF solution with stirring. Toluene is a non-solvent for the PVPh block. The presence of micelles was indicated by the appearance of turbidity in the solution. The toluene addition was continued until the desired

Macromolecular Journals
DOI: 10.1002/macp.200700078

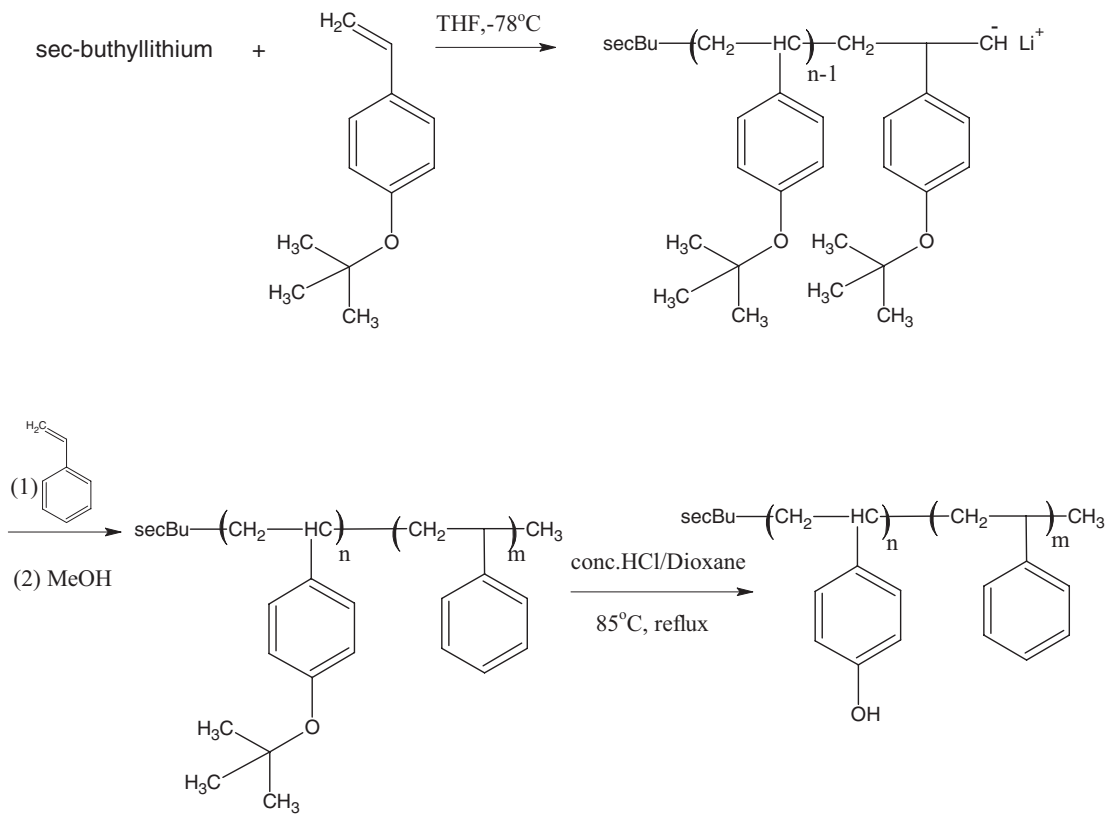

Scheme 1. Synthesis of PVPh-*b*-PS copolymer by anionic polymerization.

concentration had been reached and the THF was removed by dialysis against toluene.

Preparation of a Superhydrophobic Surface

A honeycomb structure and superhydrophobic surface consisted of PVPh cores and PS coronas were obtained by dissolving the block copolymer in THF at room temperature under stirring overnight and then slowly adding the desired amount of toluene content. The copolymer solution (20 mg · mL^{-1}) was dropped on a cleaned glass substrate under humid air (≈60 wt.-% at room temperature). After evaporation of the solvent, the morphology of the film was observed by SEM analyses.

Characterization

Molecular weight and molecular weight distribution were determined through gel permeation chromatography (GPC) using a Waters 510 HPLC equipped with a 410 differential refractometer, an RI detector, and a UV detector. Three Ultrastyragel columns (100, 500, and 10^3 Å) were connected in series and the THF was used as the eluent at the flow rate of 0.6 mL · min^{-1} and at 35 °C. The molecular weight calibration curve was obtained using polystyrene standards. ^{1}H NMR and ^{13}C NMR spectra were obtained using an INOVA 500 instrument; chloroform-*d* and 1,4-dioxane-d_8 were used as solvents. Infrared spectrum was recorded at 25 °C with a Nicolet AVATAR 320 FTIR Spectrometer using polymer film cast onto a KBr pellet from THF solution. Transmission electron microscopy (TEM) images were obtained by using a JEOL JEM-2000EXII instrument operated at 120 kV. The TEM sample was deposited from micellar solution onto a carbon-coated copper grid. After drying, the samples were stained with RuO_4. The CA of the polymer sample was measured at 25 °C using a Krüss GH-100 goniometry interfaced with image-capture software by injecting a 5 μL liquid drop.

Results and Discussion

Synthesis of PVPh-*b*-PS Copolymer by Anionic Polymerization

The block copolymer, PVPh-*b*-PS, with a total molecular weight ($\overline{M}_n$) of 18 500 g · mol^{-1} with narrow molecular weight distribution (PDI = 1.13) was designed and prepared by sequential living anionic polymerization and subsequent hydrolytic deprotection (the protected PtBOS-*b*-PS block copolymer obtained after polymerization). This diblock copolymer system has been investigated previously,[31–33] living anionic polymerization of the protected hydroxystyrene[30–35] and styrene[31–33,36] monomers is also well documented. In general, in order to obtain a monodisperse PVPh block, it is necessary to protect the hydroxyl group prior to polymerization to

avoid the termination of the living chain end. Various protecting groups, including *tert*-butyl ether[30,32,33] and *tert*-butyldimethylsilyl[31] groups have been used for hydroxyl group protection during anionic polymerization. In this study, the *tert*-butyl ether protected monomer was used because of its simple hydrolysis and ready availability.

The complete elimination of the protective groups and the regeneration of the phenolic hydroxyl group are verified by ^{1}H and ^{13}C NMR spectroscopy. Figure 1(A) and 1(B) display typical ^{1}H NMR spectra of the diblock copolymers recorded before and after deprotection. A chemical shift at 1.29 ppm corresponds to the *tert*-butyl group of the P*t*BOS-*b*-PS copolymer (in chloroform-*d*). This peak (1.29 ppm) corresponding to the *tert*-butyl group essentially disappears in the hydrolyzed block copolymer; only polymer backbone protons appear in the chemical shift region of 1–2 ppm. In addition, a peak (7.9 ppm) corresponding to the proton of the hydroxyl group appears after the hydrolysis reaction. The signal of the quarternary carbon atoms of the *tert*-butyl group in the P*t*BOS segment is located at 78.0 ppm[37] [Figure 1(C)]. After the hydrolysis reaction, no signal remains for the *tert*-butyl group at 78 ppm, indicating that the hydrolysis reaction is completed. Figure 1(D) displays the ^{13}C NMR spectra of the PVPh-*b*-PS copolymer. The FTIR spectrum of PVPh-*b*-PS (Figure 2) shows a broad peak at 3 450 cm^{-1}, indicating the presence of the OH group after deprotection. The composition of the PVPh-*b*-PS block copolymer was determined from the relative intensities of the aromatic ring and the hydroxyl group of the VPh units in the ^{1}H NMR spectrum. The signals due to the aromatic protons and the hydroxyl group were observed at 6.3–7.2 and 7.7–7.9 ppm, respectively.[32,33] and the ^{1}H NMR spectrum revealed a composition of 79 wt.-% PVPh.

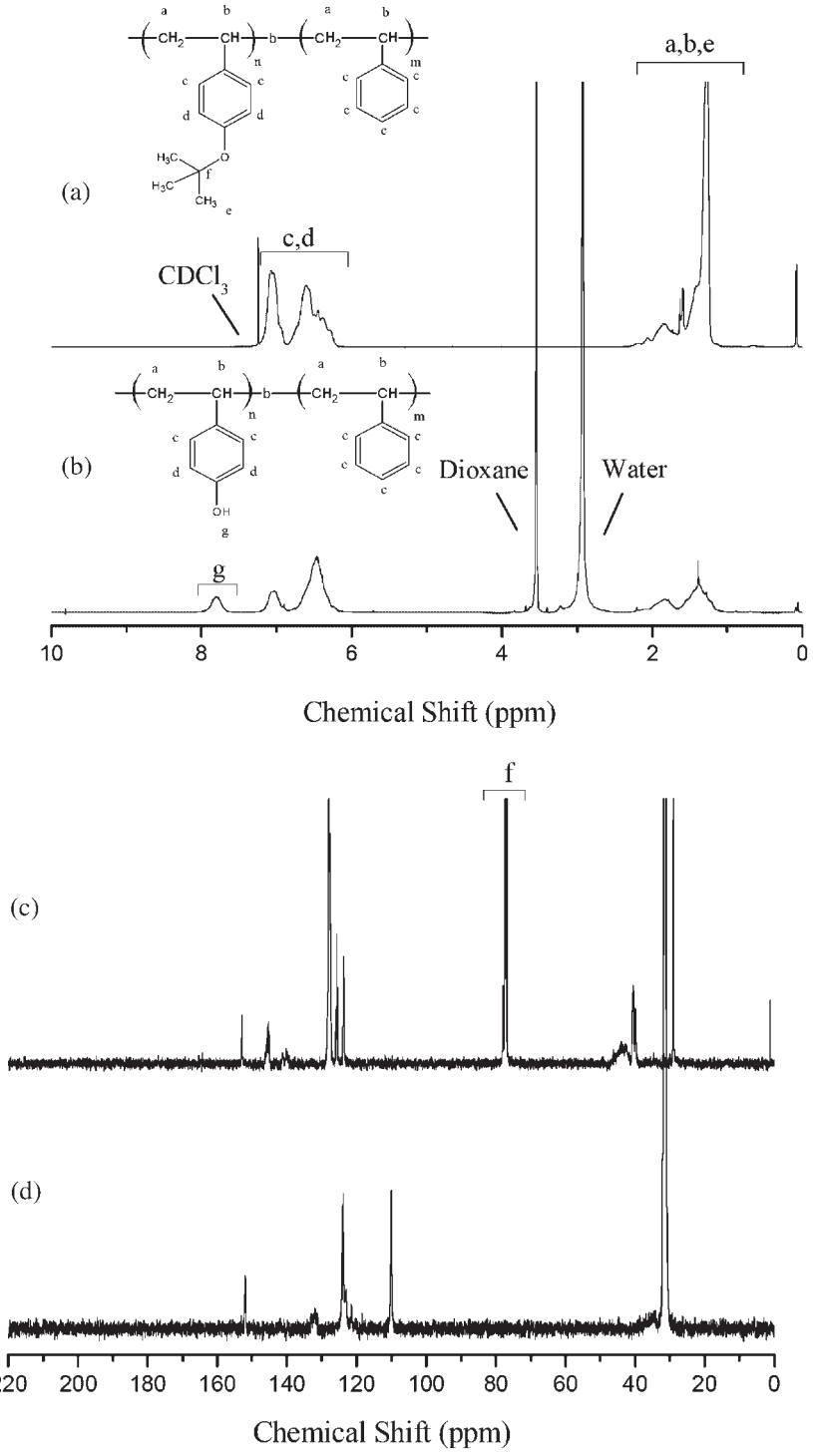

Figure 1. ^{1}H NMR spectra of P*t*BOS-*b*-PS in $CDCl_3$ (a) before and (c) after hydrolysis. ^{13}C NMR spectra of PVPh-*b*-PS in 1,4-dioxane-d_8 (b) before and (d) after hydrolysis.

Crew-Cut Micelles of PVPh-*b*-PS in THF/Toluene

The block copolymer micelle solution was prepared by adding the desirable amount of toluene slowly into the THF solution while stirring. Toluene is a fair solvent for the short length of PS block, but a non-solvent or precipitant for the long length of the PVPh block. Under this condition, the resulting micelles are expected to consist of a mildly solvent-swollen PVPh core surrounded by a corona of PS

Macromolecular Journals
DOI: 10.1002/macp.200700078

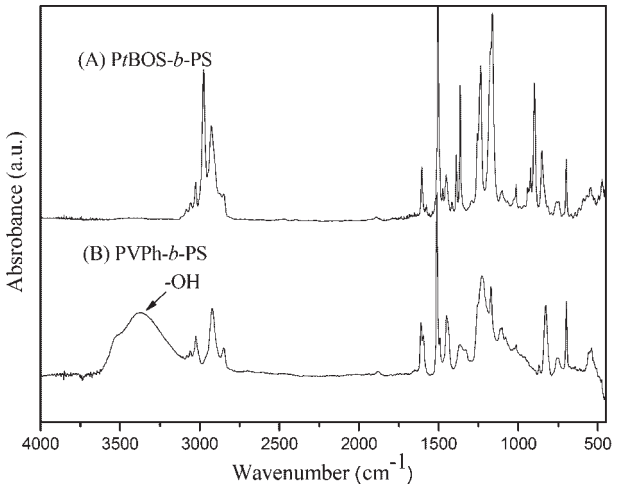

Figure 2. IR spectra of (a) P*t*BOS-*b*-PS and (b) PVPh-*b*-PS at room temperature.

blocks. Figure 3 shows various morphologies formed by this $PVPh_{79}$-*b*-PS_{21} copolymer with the same initial concentration of 2 mg · mL^{-1} in THF but different amounts of the selective toluene solvent. When toluene content is very low (0.1 mL), only spherical micelles are obtained as shown in Figure 3(A). As the selective solvent content is increased, the morphology of aggregates may change from spheres, and rods to vesicles.[38] The role of the added precipitant (toluene) on the morphology change can be described to a change in the aggregation number, which in turn influences the core dimension and the degree of stretching of the core-forming blocks. In our case, when the added toluene is at 0.15 mL, the rod-like micelles coexist with a small amount of spheres as shown in Figure 3(B). As the toluene content is at 0.25 mL [Figure 3(C)], the morphology of aggregates changes from rod-like micelles to large compound rod micelles (LRCMs). On further increasing the toluene content to 0.5 mL, vesicular aggregates begin to form; however, most of the aggregates still exist as LRCMs [Figure 3(D)]. The LRCMs have been described previously[39] and the sizes of the LRCMs are polydiperse resulting from kinetic control.[39] A mixture of vesicular and onion-like particle morphology is formed at 1 mL of toluene content as shown in Figure 3(E). These onion-like particles are in the form of a compact multi-lamellar vesicular structure,[40] which do not have a sharp contrast due to the poor selectivity stained by RuO_4 on PS and PVPh. When the toluene content is further increased to 2 mL, most of the aggregates transform into tubule and LRCM, with many small vesicles seen in the background [Figure 3(F)]. The relative low electron density of the tubules can be distinguished by their hollow structures from rods.

On the basis of the model by Shen and Eisenberg[38] the morphology of the aggregate is influenced by the added precipitant content and also by the initial copolymer concentration. When the initial concentration is more than ten-fold of 20 mg · mL^{-1}, more complicated morphologies appear. We found that the initial concentration was 20 mg

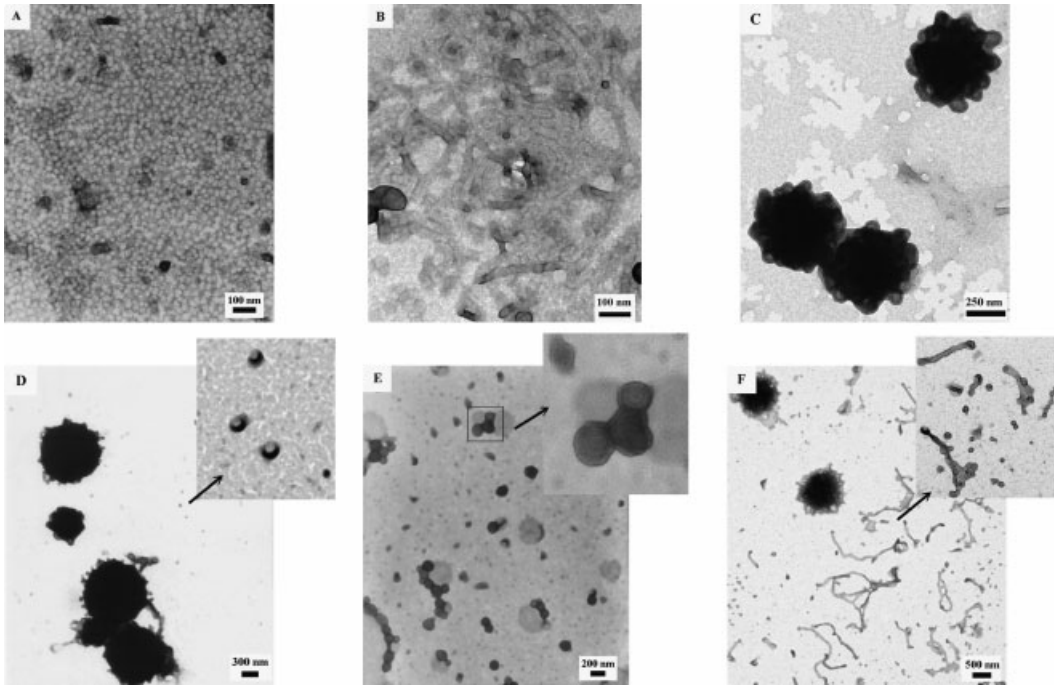

Figure 3. TEM images of 2 mg of $PVPh_{79}$-*b*-PS_{21} in 1 mL of THF with various toluene contents: (A) 0.1 mL, (B) 0.15 mL, (C) 0.25 mL, (D) 0.5 mL, (E) 1 mL toluene, and (F) 2 mL.

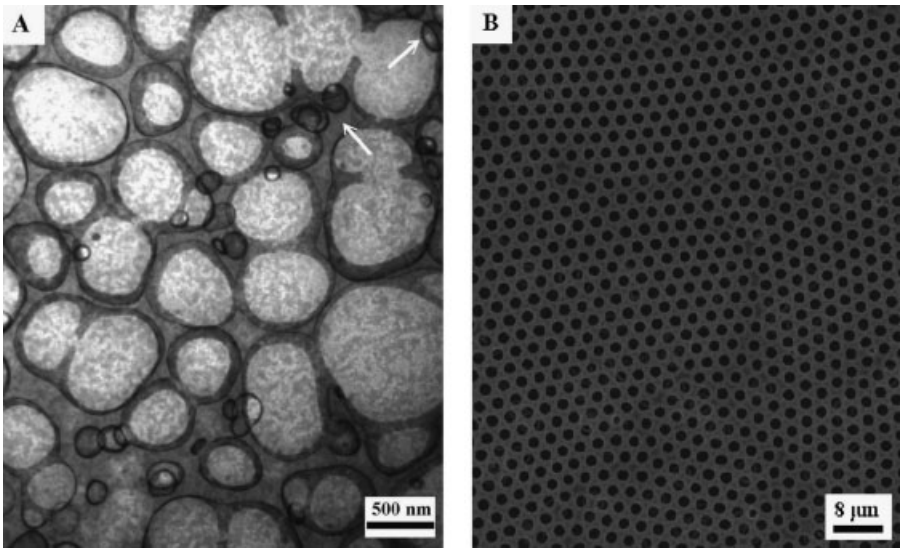

Figure 4. (A) TEM images of 20 mg of $PVPh_{79}$-*b*-PS_{21} copolymer in THF/toluene (1:0.1 v/v) and (B) the honeycomb structure of $PVPh_{79}$-*b*-PS_{21} copolymer in THF/toluene (1:0.1 v/v).

$PVPh_{79}$-*b*-PS_{21} in 1 mL of THF, and when 0.1 mL of toluene was added a fascinating morphology was observed. Figure 4(A) shows a TEM morphology for the self-assembly of $PVPh_{79}$-*b*-PS_{21} solution, which consists mainly of a perforated bilayer[41] and some vesicular aggregates appear in Figure 4(A) (see arrows in the picture). The formation of the perforated bilayer structure should involve fast adhesive vesicular aggregate collisions by a high concentrated condition and subsequently a fusion and structural rearrangement of these contacting micelles. Actually, the perforated bilayer structure,[41] and a randomly perforated lamellar phase have also been observed and discussed in PS-*b*-PAA (AA, acrylic acid) solution.[41,42] Interestingly, these vesicular aggregates, when they were cast onto solid substrates, spontaneously convert into honeycomb structures. A solvent casting film of the vesicular aggregate solution on the glass plate is prepared under a moist airflow across the solution surface. The film consists of a feature containing two-dimensional hexagonal closed packing lattice of circular holes based on SEM observation [Figure 4(B)]. Each building unit here contains a uniform hexagonal framework and each hole with diameter ca. 1 μm. Besides, the spherical shape of the porous structure reflects the shape of template water droplets. The observed honeycomb architecture is formed by the "breath figures" method.[43–56] We also discuss the honeycomb-like film's surface wettability. The water CA of the honeycomb-like film offers higher CA than the smooth surface prepared in dry atmosphere.

Now, we know that the morphology is from spheres to vesicles when the initial concentration is from 2 to 20 $mg \cdot mL^{-1}$ with the same 10 vol.-% toluene content. Meanwhile, the honeycomb-architectured films of 20 $mg \cdot mL^{-1}$ are obtained in a higher humidity atmosphere. It is very interesting to see what kinds of aggregates morphologies will be formed by increasing the toluene content in the initially high copolymer concentration (20 $mg \cdot mL^{-1}$). Here, as the toluene content reached 0.5 mL, the large porous compound micelles were formed as shown in Figure 5(A) and as the added toluene was further increased to 1 mL, these aggregates became pincushion-like micelles with a diameter of up to 2 μm, while those porous large compound micelles were still observed [Figure 5(C)]. Furthermore, the pincushion-like micelles were formed when the precipitant content was above 2 mL (toluene content 67 vol.-%) [Figure 5(D)]. The pincushion-like sphere micelles show a high polydispersity, and they cannot possibly be primary spherical micelles due to decrease in the rate of polymer chain exchange by high selective solvent content (the mechanism is kinetic control).[39,57] The diameters of the spheres formed are in the order of several hundred nanometers to several micrometers as shown by scanning electron microscopy. Figure 5(E) provides an enlarged view of these pincushion-like sphere micelles showing the spheres with protruding cylinders. Figure 6 shows the TEM images of the solvent casting film from the 20 $mg \cdot mL^{-1}$ solution containing 2 mL of toluene and then dialyzed, frozen by large toluene molecules. Figure 6(A) shows pincushion-like spheres with protruding tubular vesicles. At higher magnification, the image clearly shows giant pincushion-like spheres consisting of numerous nanotubules with an average diameter of ca. 72 nm as shown in Figure 6(B). Thus, the observed giant spheres have internal structural constituents in the form of nano-sized tubular supermicelles. The sample was stained by RuO_4 is observed as a core-shell dark/light nanotube with PS making up the shell and the PVPh the core as shown in Figure 6(B).

Here, we are not only interested in the surface patterns of $PVPh_{79}$-*b*-PS_{21} films prepared from micelle solution with different initial concentrations or precipitant contents but also the wettability of the resultant micropattern films. The wettability of these films was investigated by determining their water CAs. The smooth surface of $PVPh_{79}$-*b*-PS_{21} is only moderately hydrophobic with a water CA ca. 90°, while the $PVPh_{79}$-*b*-PS_{21} micellar aggregate films prepared in this work will enhance their hydrophobicity because of the increase in the surface

Macromolecular Journals
DOI: 10.1002/macp.200700078

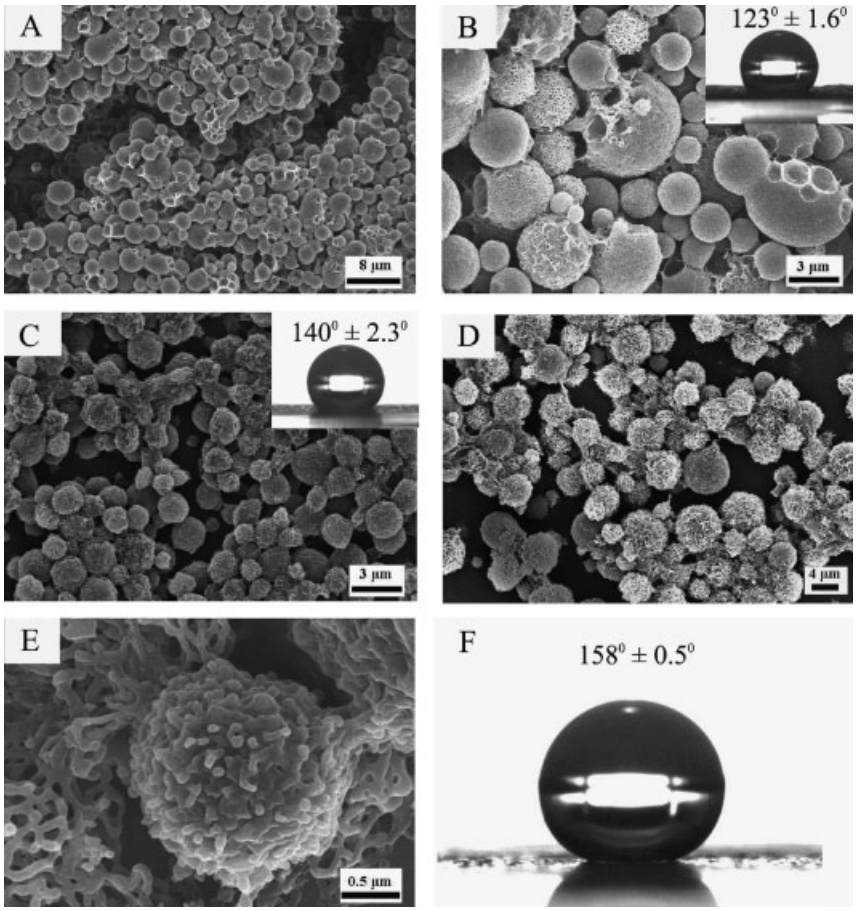

Figure 5. SEM images of the crew-cut aggregates formed by 20 mg · mL^{-1} THF solution of PVPh$_{79}$-*b*-PS$_{21}$, where the selective toluene solvent is (A) 0.5 mL, (B) enlarged view of A, (C) 1 mL, (D) 2 mL, (E) enlarged view of an individual pincushion-like micelle of (D), and (F) the CA of a 5 μL water drop on a surface of (D) pincushion-like micelles.

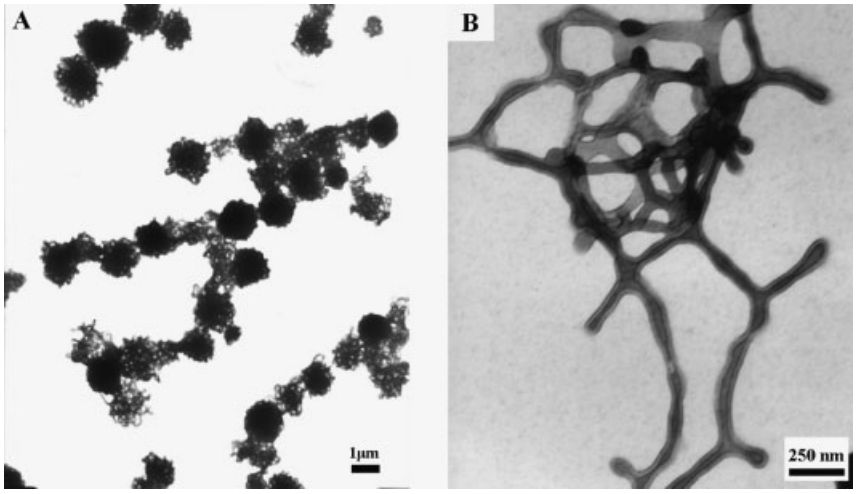

Figure 6. TEM images of 20 mg of PVPh$_{79}$-*b*-PS$_{21}$. The volume ratio of THF and toluene is 1:2. (A) The sphere with protruding tubular vesicles (LCVMs or pincushion-like micelles) and (B) enlarged image of the nanotubes shown in (A).

roughness. The PVPh$_{79}$-*b*-PS$_{21}$ micelle solution comprised an insoluble PVPh core surrounded by a soluble PS shell and was obtained by casting the PVPh$_{79}$-*b*-PS$_{21}$ block copolymer micelle solution onto clean glass substrates at room temperature. In our case, in the honeycomb-structured film of PVPh$_{79}$-*b*-PS$_{21}$, the water CA was slightly increased to 107° from 92° without toluene content due to the surface concavities of the honeycomb pores providing less polymer substrate. Furthermore, the water CA on the porous large compound micellar surface film is ca. 123 ± 1.6°. Figure 5(B) shows the enlarged view of the porous large compound micellar surface images, together with optical micrograph (inset), indicating the corresponding water CA of the film surface. The porous large compound micellar film has more surface roughness, which provides more air gaps to support the water droplet and consequently enhanced surface hydrophobicity. Most interestingly, on further increasing the toluene content to 67 vol.-% (2 mL of toluene content), the pincushion-like micellar surface film was formed and the pincushion-like sphere micelles stacking randomly on the surface made the roughness micro-scaled. Outside the tubular vesicles there are large spheres, which offer nano-scaled roughness on the coating, leading to the formation of hierarchical micro-nanoscale binary structure with a water CA ca. 158 ± 0.5° [Figure 5(F)]. The superhydrophobic property of the polymer surface and the microstructured surface of a micellar aggregate are similar to a natural lotus leaf. A bionic micro–nanoscale binary structure was also observed at a still higher toluene content, e.g., at 75 vol.-%, the morphology of 3 mL of toluene content is similar to 2 mL of toluene content, for brevity not shown here). If the difference in the aggregates' morphologies can be ascribed as an effect of selective solvent content in the copolymer solution, which induces different surface hydrophobicities as

Table 1. Summary of the structural parameters of micelles formed by $PVPh_{79}$-*b*-PS_{21} copolymer in 20 mg · mL^{-1} THF solution under different selective solvent (toluene) contents.

Selective solvent content	Morphology	CA
mL		
0	–	92
0.1	honeycomb structure	107
0.5	porous large compound micellar surface film	123
1	porous large compound + pincushion-like micellar surface film	140
2	pincushion-like micellar surface	158
3	pincushion-like micellar surface	158

summarized in Table 1. We propose that CA of the copolymer was increased from 92 to 158° by increasing the surface roughness. These phenomena can be demonstrated by Cassie's and Baxter's law[58]

$$\cos\theta_c = \gamma_1\cos\theta_1 + \gamma_2\cos\theta_2 \quad (1)$$

where θ_1 is the CA for component 1 with an area fraction γ_1 and θ_2 is the CA for component 2 with an area fraction γ_2 present in the composite material. This equation takes on special meaning when in a two-component system one component is air with a CA of 180°. With $\cos(180^\circ) = -1$, the equation reduces to

$$\cos\,\theta_c = \gamma_1(\cos\,\theta_1 + 1) - 1 \quad (2)$$

which implies that with a small γ_1 and a large θ_1 it is possible to create surfaces with a very large CA. When surface morphologies changed from smooth surface to honeycomb-structure and pincushion-like micellar structure by adjusting the toluene content, water CA increased from 92 to 107 and 158°, with total area of liquid/air surface (γ_2) increased from 0 to 0.2 and 0.92 by Cassie's and Baxter's law. From the honeycomb-structured film to the MNBS micellar structure surfaces of $PVPh_{79}$-*b*-PS_{21}, the CA is dramatically increased by changing the toluene content as shown in Figure 7. In this study, we propose that the superhydrophobic behavior can be achieved with the maximum CA of 158°, by using the pincushion-like micellar structure.

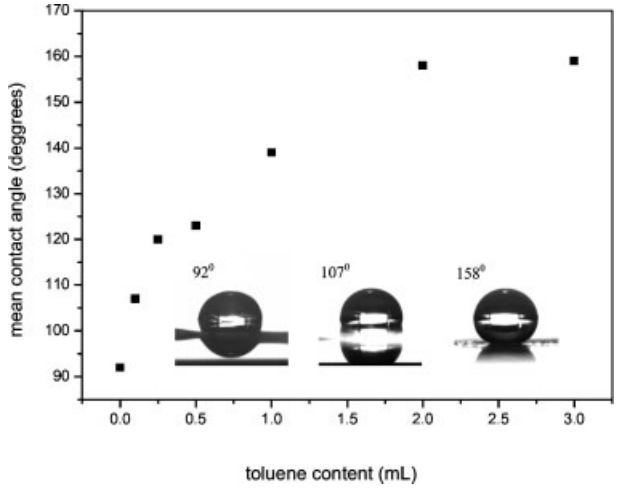

Figure 7. Water CAs of surface films by changing toluene contents.

Conclusion

Several morphologies of crew-cut aggregates were prepared from $PVPh_{79}$-*b*-PS_{21} diblock copolymers in dilute and concentrated solution including spheres, rods, vesicles, onions, tubules, porous spheres, and pincushion-like aggregates. The aggregate morphologies were controlled by the preparation process, e.g., the selective solvent content or initial concentration employed during the aggregate formation. We found that the morphology of the aggregates changes in direction from spheres to rod-like micelles and then to vesicles or bilayers. Generally, the influence of different initial concentrations on $PVPh_{79}$-*b*-PS_{21} solution is similar to different selective solvent contents. The observation of these onion-like aggregates, porous spheres, and the pincushion-like aggregate structures from a diblock copolymer provides a more difficult process of amphiphile self-assembly. We were the first to investigate high concentrated micellar solution casting onto solid matrixes, which can control the specific surface pattern of the resulting block copolymer film via changing the selective solvent content methods. When the high concentrated vesicular micellar was cast onto the glass plate under humid airflow, honeycomb-like structures were spontaneously formed. However, as the toluene content increases, porous spheres and pincushion-like aggregates were observed. The honeycomb-structured

Macromolecular Journals
DOI: 10.1002/macp.200700078

film and the microstructured surface have different values of surface roughness; moreover, they provide different water repellency. As a result, the degree of the hydrophobicity of the film could be adjusted by tuning the different toluene contents at the same concentration of the solution.

Received: February 9, 2007; Revised: May 9, 2007; Accepted: May 25, 2007; DOI: 10.1002/macp.200700078

Keywords: block copolymers; honeycomb structure; superhydrophobic surface; surfaces

[1] V. P. Torchilin, *J. Controlled Release* **2001**, *73*, 137.
[2] R. Savic, L. Luo, A. Eisenberg, D. Maysinger, *Science* **2003**, *300*, 615.
[3] C. Allen, D. Maysinger, A. Eisenberg, *Colloid Surf. B* **1999**, *16*, 3.
[4] J. Ding, G. Liu, *Macromolecules* **1997**, *30*, 655.
[5] M. Park, C. Harrision, P. M. Chaikin, R. A. Register, D. H. Adamson, *Science* **1997**, *276*, 1401.
[6] C. W. Extrand, *Langmuir* **2004**, *20*, 5013.
[7] R. Blossy, *Nat. Mater.* **2003**, *2*, 301.
[8] L. Zhang, A. Eisenberg, *Science* **1995**, *268*, 1728.
[9] L. Zhang, A. Eisenberg, *J. Am. Chem. Soc.* **1996**, *118*, 3168.
[10] B. M. Discher, Y. Y. Won, D. S. Ege, J. C. M. Lee, F. S. Bates, D. E. Discher, D. A. Hammer, *Science* **1996**, *284*, 1143.
[11] I. C. Riegel, A. Eisenberg, *Langmuir* **2002**, *18*, 3358.
[12] J. X. Zhang, L. Y. Qiu, K. J. Zhu, *Macromol. Rapid Commun.* **2005**, *26*, 1716.
[13] Y. Zheng, Y. Y. Won, F. S. Bates, H. T. Davis, L. E. Scriven, Y. Talmon, *J. Phys. Chem. B* **1999**, *103*, 10331.
[14] H. Ito, T. Imae, T. Nakamura, M. Sugiura, Y. Oshibe, *J. Colloid Interface Sci.* **2004**, *276*, 290.
[15] T. Imae, H. Tabuchi, K. Funayama, A. Sato, T. Nakamura, N. Amaya, *Colloid Surface A* **2000**, *167*, 73.
[16] T. Tao, S. Stewart, G. Liu, M. Yang, *Macromolecules* **1997**, *30*, 2738.
[17] L. Zhang, C. Bartels, Y. Yu, H. Shen, A. Eisenberg, *Phy. Rev. Lett.* **1997**, *22*, 5034.
[18] L. Desbaumes, A. Eisenberg, *Langmuir* **1999**, *15*, 36.
[19] L. Zhang, K. Yu, A. Eisenberg, *Science* **1996**, *272*, 1777.
[20] D. J. Pochan, Z. Chen, H. Cui, K. Hales, K. L. Wooley, *Science* **2004**, *306*, 94.
[21] Q. Xie, G. Fan, N. Zhao, X. Guo, J. Xu, J. Dong, L. Zhang, Y. Zhang, C. C. Han, *Adv. Mater.* **2004**, *16*, 1830.
[22] N. Zhao, Q. Xie, L. Weng, S. Wang, X. Zhang, J. Xu, *Macromolecules* **2005**, *38*, 8996.
[23] W. Bu, H. Li, H. Sun, S. Yin, L. Wu, *J. Am. Chem. Soc.* **2005**, *127*, 8016.
[24] S. R. Coulson, I. Wood, J. P. S. Badyal, S. A. Brewer, C. Willis, *J. Phys. Chem. B* **2000**, *104*, 8836.
[25] I. Woodward, W. C. E. Schofiled, V. Roucoules, J. P. S. Badyal, *Langmuir* **2003**, *290*, 2130.
[26] S. Li, H. Li, X. Wang, Y. Song, L. Jiang, D. Zhu, *J. Phys. Chem. B* **2002**, *106*, 9274.
[27] L. Feng, S. Li, Y. Li, H. Li, L. Zhang, J. Zhai, Y. Song, B. Liu, L. Jiang, D. Zhu, *Adv. Mater.* **2004**, *14*, 1857.
[28] P. H. Tung, S. W. Kuo, K. U. Jenog, C. F. Huang, S. Z. D. Cheng, F. C. Chang, *Macromol. Rapid Commun.* **2007**, *28*, 271.
[29] S. Ndoni, C. M. Papadakis, F. S. Bates, K. Almdal, *Rev. Sci. Instrum.* **1995**, *66*, 1090.
[30] M. Li, K. Douki, K. Goto, X. Li, C. Coenjarts, D. M. Smilgies, C. K. Ober, *Chem. Mater.* **2004**, *16*, 3800.
[31] J. Q. Zhao, E. M. Pearce, T. K. Kwei, H. S. Jeon, P. K. Kesani, N. P. Balsara, *Macromolecules* **1995**, *28*, 1972.
[32] E. Yoshida, S. Kungi, *J. Polym. Sci., Polym. Chem. Ed.* **2002**, *40*, 3063.
[33] E. Yoshida, S. Kungi, *Macromolecules* **2002**, *35*, 6665.
[34] P. Jannasch, *Macromolecules* **2000**, *33*, 8604.
[35] K. Se, K. Miyawaki, K. Hirahara, A. Takano, T. Fujimoto, *J. Polym. Sci., Polym. Chem.* **1998**, *36*, 3021.
[36] N. Hadjichristidis, H. Iatrou, S. Pispas, M. Pitsikalis, *J. Polym. Sci., Polym. Chem. Ed.* **2000**, *38*, 3212.
[37] C. L. Lin, W. C. Chen, C. S. Liao, Y. C. Su, C. F. Huang, S. W. Kuo, F. C. Chang, *Macromolecules* **2005**, *38*, 6435.
[38] H. Shen, A. Eisenberg, *J. Phys. Chem. B* **1999**, *103*, 9473.
[39] K. Yu, L. Zhang, A. Eisenberg, *Langmuir* **1996**, *12*, 5980.
[40] [40a] H. Shen, A. Eisenberg, *Angew. Chem. Int. Ed.* **2000**, *39*, 3310; [40b] L. Lei, J. F. Gohy, N. Willet, J. X. Zhang, S. Varshney, R. Jerome, *Macromolecules* **2004**, *37*, 1089; [40c] J. Ding, G. Liu, *Macromolecules* **1999**, *32*, 8413.
[41] L. Zhang, A. Eisenberg, *Macromolecules* **1999**, *32*, 2239.
[42] S. S. Funari, M. C. Holmes, G. J. Tiddy, *J. Phys. Chem.* **1994**, *98*, 3015.
[43] M. Srinivasarao, D. Collings, A. Philips, S. Patel, *Science* **2001**, *292*, 79.
[44] G. Widawski, M. Rawiso, B. Francois, *Nature* **1994**, *369*, 387.
[45] M. Kanehara, Y. Oumi, T. Sano, T. Teranishi, *J. Am. Chem. Soc.* **2003**, *125*, 8708.
[46] H. Yabu, M. Shimomura, *Chem. Mater.* **2005**, *17*, 5231.
[47] H. Yabu, M. Takebayashi, M. Tanaka, M. Shimomura, *Langmuir* **2005**, *21*, 3235.
[48] B. deBoer, U. Stalmach, H. Nijland, G. Hadziioannou, *Adv. Mater.* **2000**, *12*, 1581.
[49] P. S. Shah, M. B. Sigman, C. A. Stowell, K. T. Lim, K. P. Johnston, B. A. Korgel, *Adv. Mater.* **2003**, *15*, 971.
[50] C. Barner-Kowollik, H. Dalton, T. P. Davis, M. H. Stenzl, *Angew. Chem. Int. Ed.* **2003**, *42*, 3664.
[51] C. Cheng, Y. Tian, Y. Shi, R. Tang, F. Xi, *Macromol. Rapid Commun.* **2005**, *26*, 1266.
[52] U. Stalmach, B. de Boer, C. Videlot, P. F. van Hutten, G. Hadziioannou, *J. Am. Chem. Soc.* **2000**, *122*, 5464.
[53] H. Duan, M. Kuang, J. Wang, D. Chen, M. Jiang, *J. Phys. Chem. B* **2004**, *108*, 550.
[54] L. Cui, Y. Han, *Langmuir* **2005**, *21*, 11085.
[55] X. Han, J. Xu, H. Liu, Y. Hu, *Macromol. Rapid Commun.* **2005**, *26*, 1810.
[56] S. Jenekhe, X. Chen, *Science* **1999**, *283*, 372.
[57] J. X. Zhang, L. Y. Qiu, K. J. Zhu, *Macromol. Rapid Commun.* **2005**, *26*, 1716.
[58] A. B. D. Cassie, S. Baxter, *Trans. Faraday Soc.* **1994**, *40*, 546.